Chapter – 7

Mechanical Properties of Post ECAP Processed Low Carbon Steel

7.1 Mechanical properties of cold rolled ECAP-12 low carbon steel

Figure 7.1 displays the engineering stress and plastic engineering strain curves of LCS. The as-received LCS shows moderate YS of 208 MPa but highest ductility, i.e., UE of 24.9% and TE of 36.2% (Table 7.1; Figures 7.3 and 7.4). When the material is equal-channel angular pressed to ε_{vm} = 12, the UE drastically reduces to 2.1% and the TE decreases to 2.9%, though the strength increases to 872 MPa (Figure 7.1). On cold rolling of equal-channel angular pressed LCS (ECAP12-CR80), YS increases further to 924 MPa and ductility gains marginally (Table 7.1). Flash annealing of the ECAP12-CR80 sample at 853 K (580°C) leads to a decrease in the YS to 520 MPa, but the UE increases to 11.2% (Figure 7.1; Table 7.1). Further flash annealing of the ECAP12-CR80 at 873 K (600°C) leads to a decrease in the YS to 484 MPa, which is still twice that of as-received LCS; importantly the TE and UE increase to 23.3 and 17.4%, respectively (Figure 7.1).

There is no undulation in the tensile plot of as-received LCS, but it is significant in ECAP12-CR80-FA580 and ECAP12-CR80-FA600. Table 7.1 gives the area under the stress-strain curve or absorbed energy, which is directly related to tensile toughness. It is maximum (137 MJ/m3) in the as-received LCS. It decreases drastically to a low value (27 MJ/m^3 for ECAP-12 and 46 MJ/m^3 for ECAP12-CR80) for the UFG material. On annealing, it increases (86 MJ/m^3 for ECAP12-CR80-FA580 and 112 MJ/m^3 for ECAP12-CR80-FA600). The as-received material shows a low hardness value of 158 ± 6 VHN (Figure 7.2; Table 7.1). On ECAP for ε_{vm} = 12, the hardness value increases drastically to 411 ± 6 VHN. When the ECAP12 sample is deformed further by cold rolling to 80% reduction in area, hardness increases further to 467 ± 6 VHN. On annealing at 853 K (580°C) for ECAP12-CR80 samples, the hardness decreases to 334 ± 8 VHN. When the equal-channel angular pressed, and cold-rolled material is flash annealed at 873 K (600°C), hardness further decreases to 308 ± 9 VHN. The ratio of Vickers hardness to YS is highest (7.56) for as-received material. On deformation, the ratio decreases, but it increases again by flash annealing (Table 7.1).

Table 7.1: Mechanical properties of deformed and annealed low carbon steels

Sample	YS (σ_y) (MPa)	UTS (σ_{UTS}) (MPa)	Plastic U E (%)	Plastic T E (%)	Hardness (H_v) (VHN) Kg/mm^2	Ratio $H_v/\sigma_{y/10}$ unitless	Absorbed energy before farcture (MJ/m^3)
As-received	272	367	22	41	159±4	7.56	137
ECAP12	872	996	2.2	2.9	459±6	4.7	27
ECAP12-CR80	924	1104	2.7	4.5	467± 6	5.0	46
ECAP12-CR80-FA580	520	560	11.2	16.2	334±8	6.42	86
ECAP12-CR80-FA600	484	517	17.5	23.3	308±9	6.36	112

Yield strength (YS), ultimate tensile strength (UTS), total elongation (TE) and uniform elongation (UE).

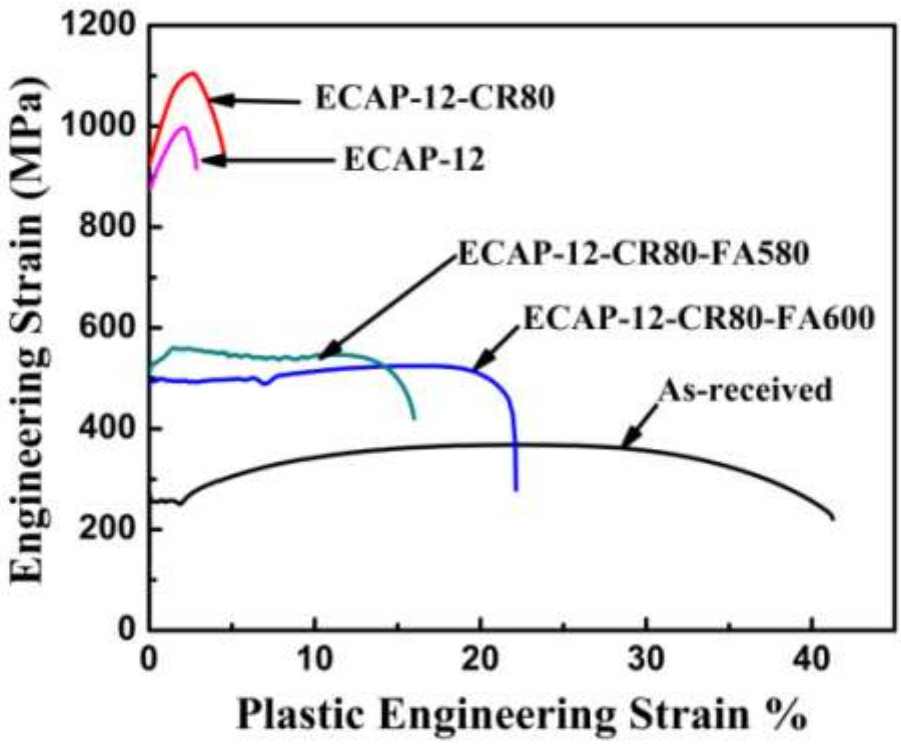

Figure 7.1: Engineering stress and plastic engineering strain of low carbon steels.

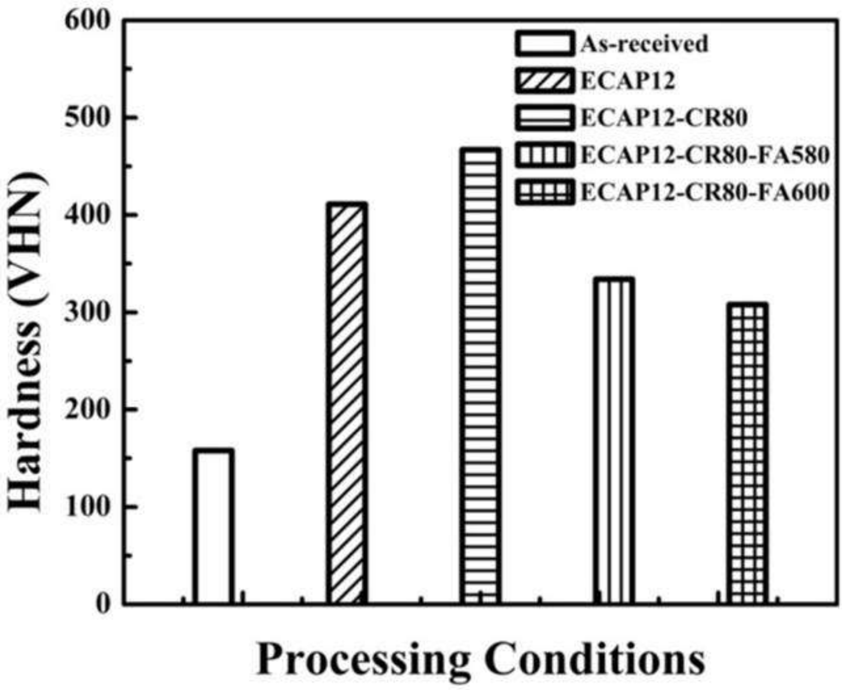

Figure 7.2: Variation of hardness with processing conditions.

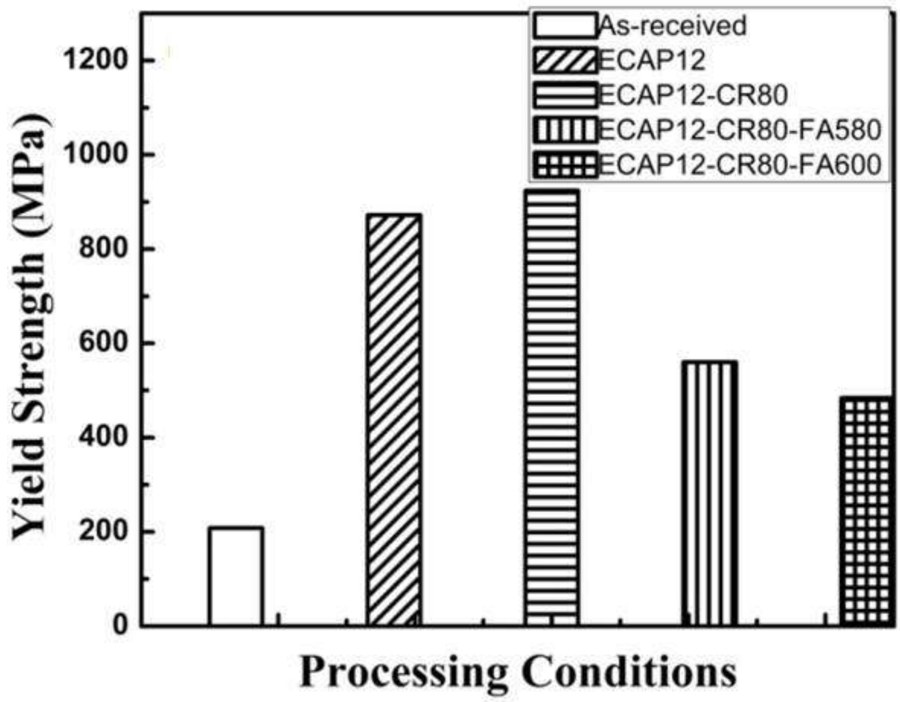

Figure 7.3: Variation of hardness with processing conditions.

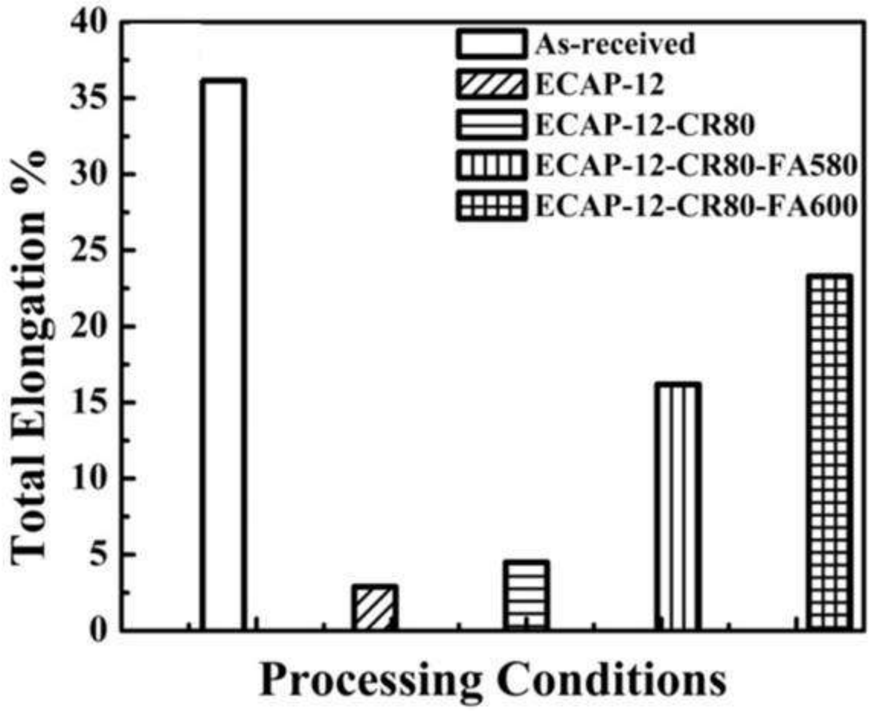

Figure 7.4: Variation of hardness with processing conditions.

7.2 Mechanical Properties of Cryo-Rolled ECAP-16.8 Low Carbon Steel

Figure 7.5 displays the Engineering stress vs. engineering plastic strain plots of deformed and annealed low carbon steel samples. The as-received low carbon steel has UTS of 368 MPa with high ductility, i.e., uniform elongation 23% and total elongation of 41%. When the material is ECAPed to ε_{vm}=16.8, the UTS increases to 1008 MPa (Figure 7.5), and the uniform elongation reduces drastically to 1%. At the same time, the total elongation decreases to 10.6%. On cryo-rolling of ECAPed low carbon steel (ECAP-16.8-CRR-75), ultimate tensile strength increases further to 1238 MPa but the total elongation reduces to 4.6% (Table 7.2). When ECAP-16.8-CRR-75 samples are flash annealed at 600ºC UTS decreases to 488. However, ductility is recovered with uniform elongation of 20% and total elongation of 25% (Table.7.2).

Figure 7.6(b) represents variation in Vickers hardness of deformed low carbon steel with annealing temperature. As-received hot rolled low carbon steel is having the Vickers hardness value of 1588±80 MPa. After ECAP for ε_{vm}=16.8 (ECAP-16), the hardness increases to 4527±60 MPa. When deformation mode is changed from ECAP to ECAP+cryo-rolling, the hardness of the material is increased to 4831±90 MPa. When the cryo-rolled samples are annealed at 475°C, the hardness begins to decrease to 4077±40 MPa. At 500°C, the hardness of the deformed samples reaches 3724±100 MPa and a further decrease to 3322±70 MPa when flash annealing temperatures goes upto 550°C. The hardness continues decrease with increasing flash annealing temperature at 600°C it reaches 3175±70 MPa. The hardness continues decrease with increasingly flash annealing temperature, and a 675°C, to a low value of 2744±60 MPa (Figure 7.6).

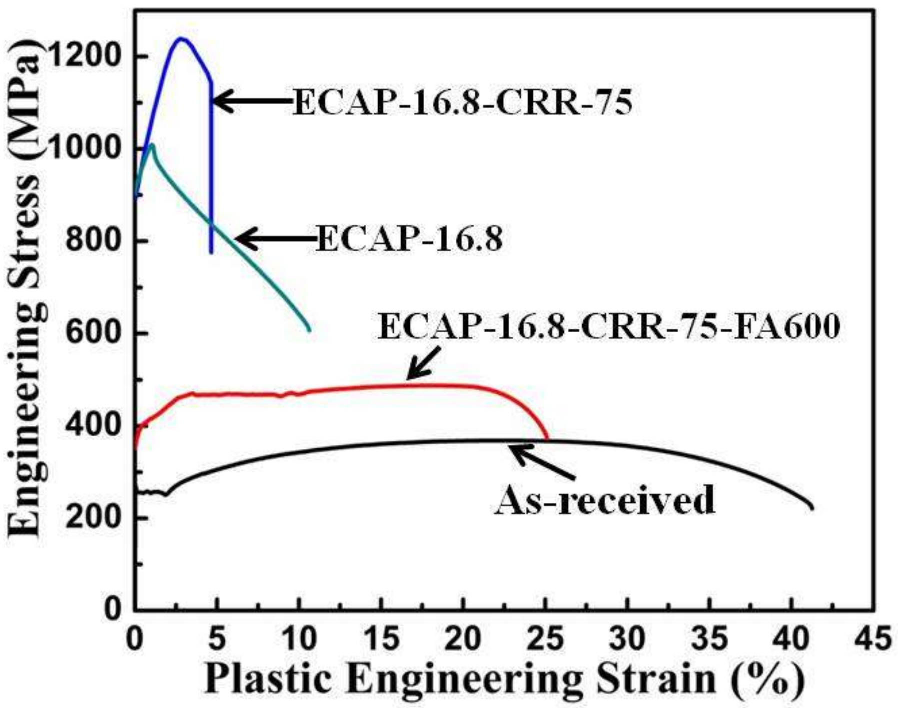

Figure 7.5: Engineering stress vs engineering plastic strain plot of low carbon steel samples.

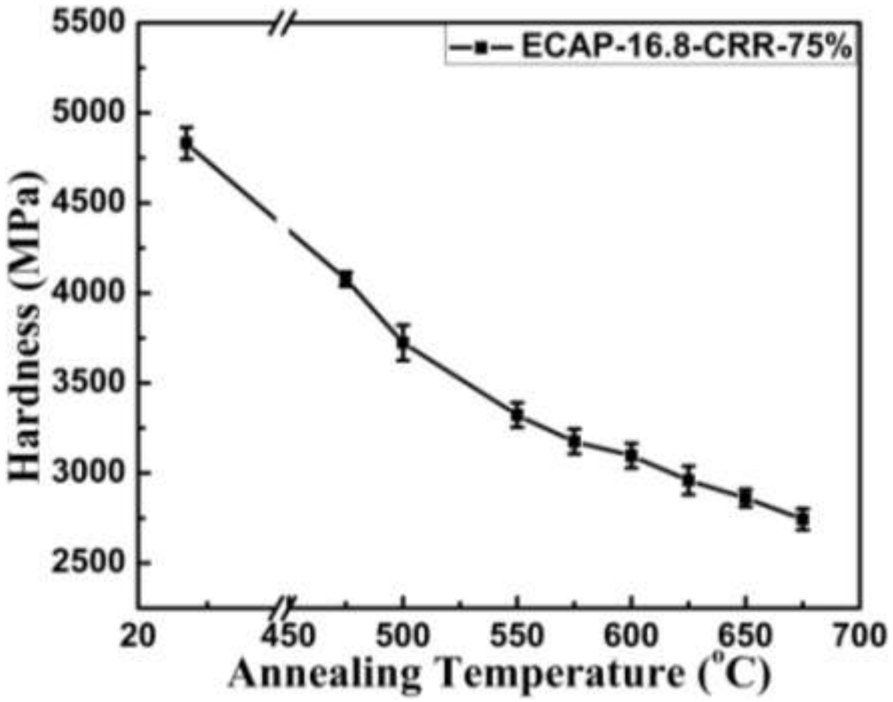

Figure 7.6: Variation of hardness value with flash annealing temperature of deformed sample (ECAP-16.8-CRR-75.

Table 7.2: Mechanical properties of low carbon steels processed by ECAP followed by cryo-rolling and flash annealing.

Sample	YS, MPa	UTS, MPa	Uniform Elongation, %	Total Elongation, %
As-received	272	368	22	41
ECAP-16.8	902	1008	1	10.6
ECAP-16.8-CRR-75	890	1238	2.7	4.6
ECAP-16.8-CRR-75-FA600	351	488	20	25

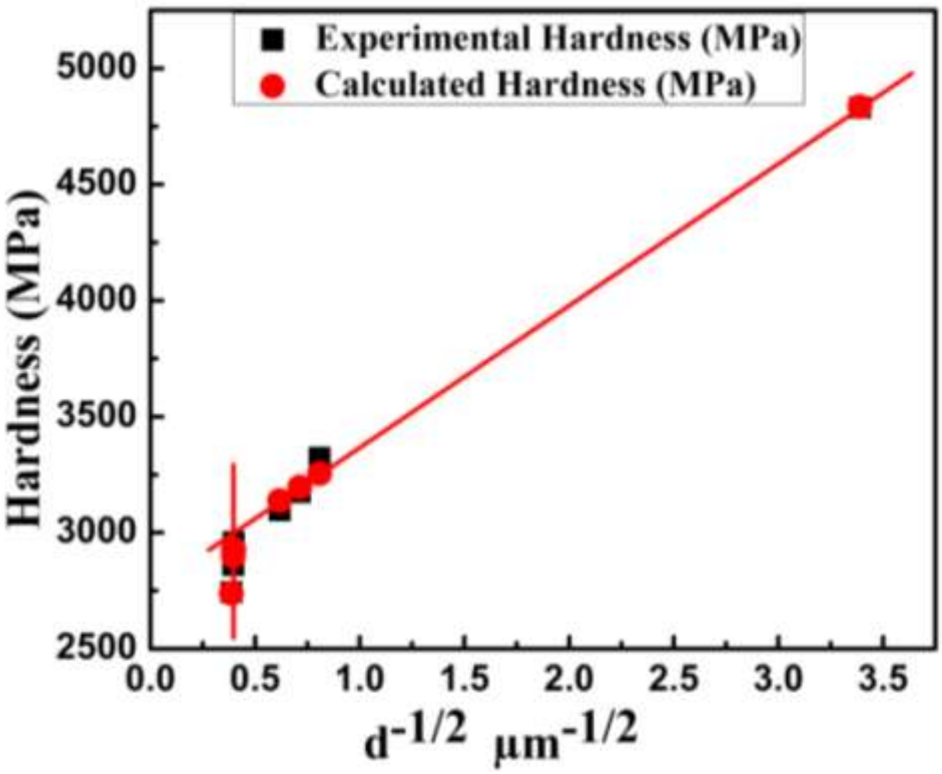

Figure 7.7: Variation of hardness with inverse square root of grain size ($d^{-1/2}$) of ECAP-16.8-CRR-75-FA.

A linear fit is made from the experimental values of hardness and an inverse square root of grain size in two-temperature ranges- one below 600°C and other one above 625°C. Values for the H_o and K in low temperature range are 2760.5MPa and

611.9MPa $m^{1/2}$ respectively, and the curve is designated A. In the higher temperature range the fitted curve is designated as B, and the values of Ho and K are 4310.6MPa & 18226MPa$m^{1/2}$ respectively in the latter case. There is a change in gradient of the fitted curve at 600°C (Figure 7.7).

7.3 Fractography

The fractograph of as-received LCS shows the presence of large dimples of average size 37 ± 6 µm throughout the area (Figure 7.8(a); Table 7.3). The presence of large size dimples is indicative of ductile fracture and less stored energy (45 J/mol) in the material (Table 7.3). As the material is equal-channel angular pressed for ε_{vm} = 12, the material fails by the cleavage fracture on tensile testing. The fractograph displays 38% area of cleavage fracture and the rest of the area as ductile fracture with dimple size of 3.6 ± 2 µm. The stored energy is increased to 145 J/mol (the cleavage area is shown by the arrow in Figure 7.8(b)). The fractograph of ECAP12-CR80 contains only 15% fine elongated dimples of size 2.3 ± 1.5 µm, with the rest of the area filled by cleavage regins mode (elongated dimple shown by double arrows in sample ECAP12-CR80, Figure 7.8(c)). Stored energy at this stage decreases to 93 J/mol due to recovery taking place during cold rolling (Table 7.3). When the ECAP12-CR80 samples are flash annealed at 873 K (600°C), the fracture behavior changes. The ductile area increases to 79% and the size of the dimples increase to 17 ± 5 µm.

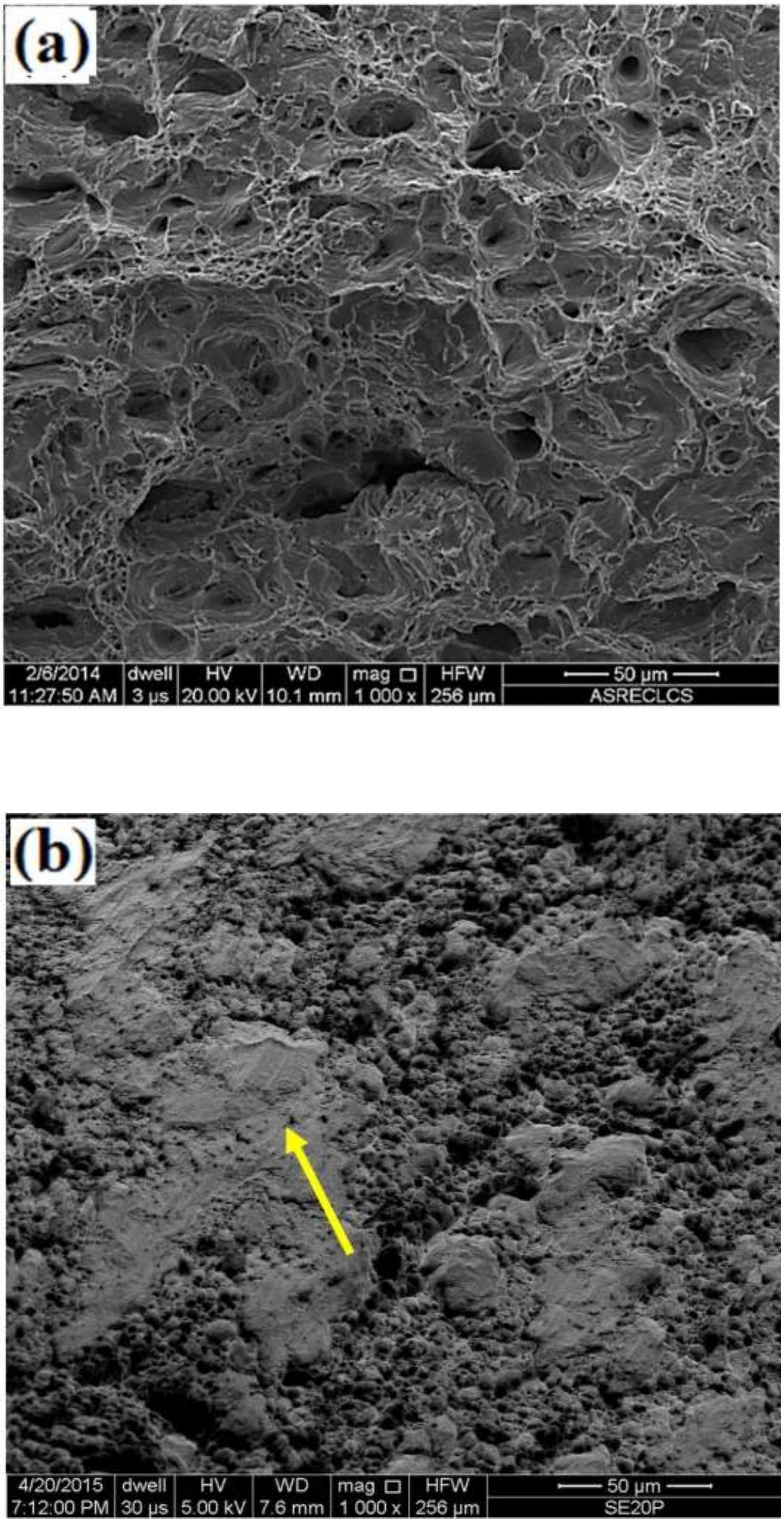

Figure 7.8: Fractographs of LCS: (a) as received, and (b) ECAP12, The single arrow indicates the cleavage area.

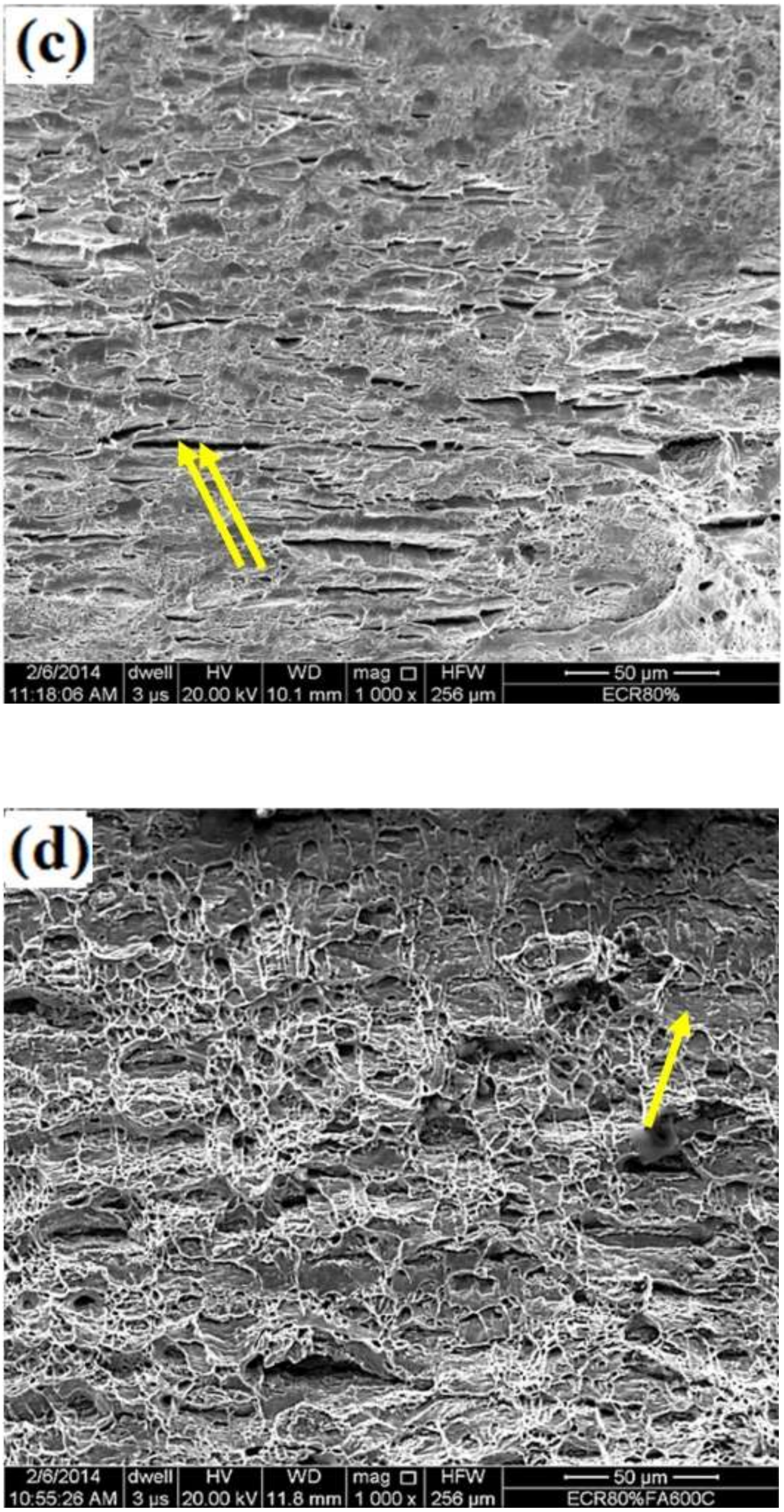

Figure 7.8: Fractographs of LCS: (c) ECAP12-CR80, and (d) ECAP12-CR80-FA600. The single arrow indicates the cleavage area, and the double arrows show elongated crack.

Even though the dimple size is lower than that of the as-received sample (Figure 7.8(d)), it is higher than that of cold rolled sample, ECAP12-CR80; as a result, the ductility of the annealed material is recovered significantly (cleavage area is shown by the single arrow in Figure 7.8(d)). Stored energy decreases to 55 J/mol (Table 7.3).

Table 7.3: Size and area fraction of dimple and cleavage areas in low carbon steel

Sample	Dimple Area %	Dimple size (μm)	Cleavage Area %	Stored Energy J/mol
As-received	100	37±6	-	45
ECAP12	62	3.6±2	38	145
ECAP12-CR80	15	2.3±1.5	85	93
ECAP12-CR80-FA600	79	17±5	21	55
ECAP12-CR80-FA580				69

7.4 Discussion

The equal-channel angular pressed LCS sample has a saturated dislocation density; when the deformation mode changes from ECAP to ECAP+rolling, part of the dislocations rearrange to lower energy configurations, which reduces dislocation density, but the reductions in both cell size and grain size enhance hardness as well as strength. Therefore, when the ECAP12 material is cold rolled, the tensile strength increases due to further grain refinement and low mobile dislocations. The UFG material lacks dislocation interactions, which produces a very low strain-hardening rate. Consequently, plastic instability occurs at very early stages of tensile testing, displaying a limited UE [Purcek et al. 2012]. When the material is deformed by the ECAP process, hardness increases due to decrease in the grain size, increase in the fraction of the HAGBs, and high dislocation density. Hardness increases further when the deformation mode changes from ECAP to ECAP+rolling. This increase is due to further grain refinement and a large number of accumulated dislocations.

On annealing ECAP12-CR80 sample at 853 K(580°C), the UTS drops down, and the TE increases due to recrystallisation and coarsening of micron-sized grains by abnormal grain growth or secondary recrystallisation [Humphreys et al. 1995]. On the other hand, the YS is still 2.5 times that of the as-received LCS, which is the result of presence of high fraction of ultrafine grains (Figure 7.1), HAGBs (Figure 6.5(f)), and a good amount of dislocation density. As the annealing temperature increases to 873 K(600°C), the area fraction of coarse grains increases to 27%, which leads to a minor drop in strength but an increase in UE to 17%. The high defect density allows sufficient nucleation during recrystallisation at the elevated temperature so that a significant amount of ferrite grains remain in the ultrafine-grain range in the matrix to maintain the high strength of the material. Micrometer size grains obtained through secondary recrystallisation produce pronounced strain hardening to sustain useful uniform deformation [Berbenni et al. 2007]. Serrations appear in the stress–strain curve, possibly due to dynamic strain aging. This is pronounced in severely deformed LCS but less so in the annealed material at room temperature. Therefore, these undulations are absent in the as-received sample, less in ECAP12- CR80-FA600, but more in ECAP12-CR80-FA580. Undulations or serrations due to dynamic strain aging were reported in severe plastically deformed UFG carbon steel by many authors at room temperature [Antolovich et al. 2014]. As usual expected, annealing of equal-channel angular pressed and cold-rolled LCS reduces hardness due to recrystallisation. Hardness decreases with increasing annealing temperature, but the ratio of Vickers hardness and yield tensile strength of the annealed material remains constant—a function of the material itself. For the annealed material, the ratio is highest, and it decreases with deformation [Zhang et al. 2011]. The trend of the ratio of the experimental material matches the earlier findings for other materials such as Cu and Cu-Zn alloys [Zhang et al. 2011].

In the present work, on the ECAP of low-carbon pearlitic steel of average interlamellar spacing of 220 nm, partial dissolution of cementite plates takes place, which leads to a reduction of the average spacing of pearlite (<100 nm, Figure 6.1(a)). Cold rolling of equal-channel angular pressed LCS to 80% reduction in area enhances further dissolution of carbides. Flash annealing of ECAP12-CR80 at 853 K results in the bimodal distribution in ferrite grain size (Figures 6.3(a) through (d)) with a small amount of precipitation of cementite particles of size 15 to 20 nm (Figure 6.3(e)). However, the ductility of the steel improves marginally compared to that of the deformed material (Table 7.1). The UE increases from 2.7 to 11.2%, and the TE improves from 4.5 to 16.2%. When the LCS of ECAP12-CR80 is flash annealed at 873 K (600°C), a small number of cementite particles of size 35 to 50 nm are precipitated but the volume fraction of coarse grains increases to 27% (Figure 6.4(d)). There is a significant improvement in both UE and TE (Table 7.1). The UE improves from 2.7 to 17.5%, and TE enhances from 4.5 to 23.3%. Therefore, a major contribution towards ductility comes from the bimodal grain size distribution of ferrite rather than the precipitation of cementite.

ECAP of low carbon steel increases strength as well as hardness to ultra high level due to the refinement of the material to ultrafine level with a significant amount of defect density. On cryo-rolling of ECAPed low carbon steel the grain size reduces to nanometer level with higher defect density and non-equilibrium nature of boundaries due to restricted recovery at subzero temperature. This leads to further strengthening and hardening of the material. However, nanostructure low carbon steel loses its ductility due to less work hardening ability of grains of non-equilibrium nature of boundaries.

On flash annealing of ECAPed and cryo-rolled low carbon steel at low temperature (<500°C) the material is recovered. Therefore hardness decreases marginally. When the steel is flash annealed above 550°C, the material undergoes partly recrystallisation and partly secondary recrystallisation. Therefore, significant drop in hardness could be observed. Flash annealing above 600°C leads to secondary recrystallisation that results in bimodal grain size distribution. Material loses its strength but recovers ductility significantly. The fine grains offer strength, but coarse grains provide ductility to the material. Below 600°C, strengthening is due to grain refinement, high defect density and non-equilibrium nature of grain boundaries but above 600°C, strengthening is due to fine grain size. Because of change in the mechanism of strengthening in two ranges of flash annealing temperature, change in gradients could be observed in the plot of hardness vs. inverse square root of grain size.

The fracture surface of the as-received LCS has a low elastic stored energy, and coarse dimples on fracture surface are indicative of the ductile fracture that causes the UE to be high. The SPD by ECAP results in the UFG structure with high dislocation density and high elastic stored energy (Table 7.3). In equal-channel angular pressed LCS, the energy required for nucleation of dimples is more than that of their growth and coalescence [Tarpani et al. 2002]; because of this, the material fails by cleavage fracture on tensile testing. The material depicts extremely low ductility in the ECAP12-CR80 sample. Some of the dimples become elongated due to elongated grain structures, and a few remain equiaxed due to scattered equiaxed grain structures. Moreover, a fractograph displays a large fraction of cleavage fracture area (indicated by a single arrow in Figure 7.8(c), which signals the brittleness of material even though ductility increases marginally. Flash annealing of ECAP12-CR80 at 873 K (600°C) releases the elastic stored energy. Therefore, the fracture surface shows mixed facets and a dimpled surface (Figure 7.8(d)), which is designated as the quasi-cleavage fracture. This fracture can be attributed to the ultrafine new recrystallized grains as well as the abnormally grown coarse grains at the higher temperature. There is the appearance of cleavage facets, which are formed due to reinitiation of the cleavage fracture at the new grain boundaries having a high angle of misorientation. A visual inspection shows that the dimples become deeper and their average lateral size is increased. The increased dimension of dimples indicates the regaining of ductility, and the material fails by quasi-cleavage fracture.

The area under the stress–strain curve or absorbed energy, which is also directly related to the tensile toughness, is maximum in the as-received LCS because of the coarse-grained structure from the hot-rolled condition. It decreases drastically to a low value for UFG material produced by ECAP and ECAP followed by cold rolling. The decrease is due to the high defect density and nonequilibrium nature of grain boundaries in the UFG material. Annealing of UFG steel processed by ECAP and ECAP followed by cold rolling, toughness increases due to the annihilation of defects and the equilibrium nature of boundaries. Enhancement in toughness is observed in UFG LCS processed by the warm rolling/ accumulative roll bonding/thermomechanical non-recrystallisation control process for similar reasons that the UFG structure (grain size 0.5 to 5 μm) with low defect density decreases the impact transition temperature and increases impact energy [Safarov et al. 2014, Tsuji et al. 2004, Leinonen 2004].

The desirable texture for good ductility is formation of γ fiber or orientation of maximum fraction of grains with {111} planes parallel to the deformation plane or slip plane [Haldar et al. 2009, Ray et al. 1994, He 2013]. The as-received material has a high intensity of γ fiber component $(111)[1\bar{2}3]$. Therefore, the as-received material shows high ductility. On ECAP, the texture component $(110)[1\bar{1}1]$ of intensity 3.2 is developed. Therefore, ductility decreases to a low level. On cold rolling of equal-channel angular pressed LCS, strong γ fiber components $(111)[1\bar{1}1]$ and $(111)[1\bar{1}0]$ of respective intensities 20.8 and 5.3 form and are helpful in recovering some amount of ductility. After annealing at 853 K (580°C), the ductility improves due to the development of a new γ fiber component $\{111\}[0\bar{1}1]$ of maximum intensity 3.8 but the intensities of the α fiber component $(001)[1\bar{1}0]$ and the existing component $(001)[1\bar{1}0]$ remain almost unchanged. When equal-channel angular pressed+cold-rolled material is annealed at 873 K (600°C), a good amount of γ fiber components (111)[110] and $(111)[\bar{1}\bar{4}5]$ reappear in addition to the new component that becomes shifted to $(001)[\bar{1}\bar{2}0]$; as a result, the material recovers ductility significantly. When the material exhibit strong texture, most of the boundaries between the two adjacent grains are of a low angle of misorientation, which leads to low mobility of the boundaries.

7.5 Summary

Grain refinement in ultrafine level after cold rolling of ECAP-12 and high dislocation density provide ultrahigh strength (YS> 900 MPa) but reduces ductility, and the material fails by cleavage fracture due to development of a $(110)[1\bar{1}1]$ texture component at the expense of a γ fiber component of $(111)[1\bar{2}3]$.

Ultimate tensile strength of bulk nanostructured steel increases to 1238 MPa after cryo rolling of ECAP-16.8. The ductility of the material is drastically dropped due to high defect density and non-equilibrium nature of boundaries of nano-grains.

ECAP followed by cryo-rolling and flash annealing of low carbon steel produces a novel microstructure of bimodal grain size distribution of ultrafine-grains and micron-sized-grains due to the combination of recrystallisation and secondary recrystallisation respectively. The bimodal structure recovers ductility from micron-sized grains whereas ultrafine-grains carry the strength. Therefore ECAP combined with cryorolling and flash annealing can be utilized to get both high with high ductility. However, the material is partially recrystallised because of the short period of annealing.

Flash annealing at 873 K (600°C) of LCS develops required bimodal grain size distribution in ferrite (73% volume of fine grains of size 0.8µm and 27% volume of coarse grains of size 9µm) with a small amount of fine cementite precipitates, where ductility is recovered due to the optimum quantity of micron-sized ferrite grains and precipitates with development of a good amount of γ fiber texture components of (111)[110] and (111)[$\bar{1}\bar{4}$5].

Ductility of UFG LCS can be recovered by a combination of ECAP followed by cold rolling and suitable flash annealing, where a major contribution toward ductility comes from bimodal grain size distribution in ferrite rather than precipitation of cementite. The ultrafine ferrite grains are failed by cleavage fracture, but the micron-sized grains permit ductile fracture.